

---

# Learning the Plasticity: Plasticity-Driven Learning Framework in Spiking Neural Networks

---

Guobin Shen<sup>1,3\*</sup>, Dongcheng Zhao<sup>1\*</sup>, Yiting Dong<sup>1,3</sup>,  
Yang Li<sup>1,4</sup>, Feifei Zhao<sup>1</sup>, Yi Zeng<sup>1,2,3,4†</sup>

<sup>1</sup> Brain-inspired Cognitive Intelligence Lab, Institute of Automation, Chinese Academy of Sciences

<sup>2</sup> Center for Excellence in Brain Science and Intelligence Technology, CAS

<sup>3</sup> School of Future Technology, University of Chinese Academy of Sciences

<sup>4</sup> School of Artificial Intelligence, University of Chinese Academy of Sciences

{shenguobin2021, zhaodongcheng2016, dongyiting2020,  
liyang2019, zhaofeifei2014, yi.zeng}@ia.ac.cn

## Abstract

The evolution of the human brain has led to the development of complex synaptic plasticity, enabling dynamic adaptation to a constantly evolving world. This progress inspires our exploration into a new paradigm for Spiking Neural Networks (SNNs): a Plasticity-Driven Learning Framework (PDLF). This paradigm diverges from traditional neural network models that primarily focus on direct training of synaptic weights, leading to static connections that limit adaptability in dynamic environments. Instead, our approach delves into the heart of synaptic behavior, prioritizing the learning of plasticity rules themselves. This shift in focus from weight adjustment to mastering the intricacies of synaptic change offers a more flexible and dynamic pathway for neural networks to evolve and adapt. Our PDLF does not merely adapt existing concepts of functional and Presynaptic-Dependent Plasticity but redefines them, aligning closely with the dynamic and adaptive nature of biological learning. This reorientation enhances key cognitive abilities in artificial intelligence systems, such as working memory and multitasking capabilities, and demonstrates superior adaptability in complex, real-world scenarios. Moreover, our framework sheds light on the intricate relationships between various forms of plasticity and cognitive functions, thereby contributing to a deeper understanding of the brain's learning mechanisms. Integrating this groundbreaking plasticity-centric approach in SNNs marks a significant advancement in the fusion of neuroscience and artificial intelligence. It paves the way for developing AI systems that not only learn but also adapt in an ever-changing world, much like the human brain.

## 1 Introduction

Synaptic plasticity, characterized by the ability of synapses to strengthen or weaken over time, underpins learning and memory in the human brain. This adaptive mechanism allows for dynamic responses to an ever-evolving environment, manifesting across various levels from molecular to neural networks [1; 2; 3; 4]. Its significance is widely recognized; however, the direct application of synaptic plasticity as an optimization algorithm in artificial neural networks presents notable challenges.

One of the key challenges arises from the diversity of learning rules observed in biology, such as Long-Term Depression (LTD), Long-Term Potentiation (LTP), and Spike-Timing-Dependent Plasticity

---

\*Equal contribution.

†Corresponding Author.

(STDP). These mechanisms, although instrumental in understanding and implementing functions like learning and memory, are often challenging to directly apply in neural network optimization due to their complexity and subtlety [5; 6; 7; 8]. Traditional modeling methods, inspired by biological evidence, struggle to capture the inherent dynamism of neural systems and require meticulous hand-design or integration with deep learning optimization techniques.

Spiking Neural Networks (SNNs) adeptly emulate the discrete spike sequence information transmission found in biological nervous systems, intricately modeling the dynamics of biological neurons. The intrinsic event-driven and real-time nature of information processing in SNNs grants them an enhanced capability for managing tasks with temporal dynamics, outperforming traditional Artificial Neural Networks (ANNs) in these aspects [9]. While backpropagation has been established as a foundational technique in neural network optimization [10; 11], its precise analog in biological systems remains controversial, raising questions about the feasibility of replicating complex biological tasks using such algorithms [12]. Another way to optimize SNNs is to draw on plasticity mechanisms in biology. This approach replicates the challenges of complex tasks based on local synaptic plasticity rules observed in biological systems. However, enhancing the learning ability of SNN through various learning rules often relies on the coordination of manual presets and lacks the flexibility to adapt to changes in different environments [13; 14; 15], limiting the development of this field.

We argue that the main challenge in this field stems from the rigid application of observed biological plasticity mechanisms in neural network design. There is a lack of abstraction and deeper understanding of these mechanisms, leading to models that do not fully exploit the adaptability and learning potential of synaptic changes. To overcome these limitations, we propose an innovative approach that shifts the focus from traditional synaptic weight adjustments to learning the principles of plasticity. We advocate for an abstract and parametric modeling of plasticity, aiming to learn and adapt the rules of plasticity within the network. This paradigm shift aligns more closely with the dynamic nature of biological learning and opens avenues for developing more robust and adaptable neural network models.

Our contributions can be summarized as follows:

- We propose abstract and parametric modeling of biological plasticity, providing a higher level of generalization and summary of local plasticity, leading to more flexible forms and better generalization capabilities.
- We introduce the Plasticity-Driven Learning Framework (PDLF), emphasizing the understanding and application of plasticity rules over traditional synaptic weight adjustments, allowing neural networks to evolve and adapt in dynamic environments.
- This approach potentially enhances the generalization and multitasking abilities of SNNs in dynamic and real-world scenarios, offering a platform for continuous learning and adaptation, mirroring the extraordinary capabilities of biological nervous systems.

## 2 Results

### 2.1 Plasticity-Driven Learning Framework

The realm of Spiking Neural Networks (SNNs) has witnessed the identification of multiple local plasticity mechanisms, such as Spike-Timing-Dependent Plasticity (STDP) [3] and Bienenstock-Cooper-Munro (BCM) rules [16]. However, abstracting and refining these biological observations into concrete plasticity mechanisms suitable for diverse complex tasks remains a formidable challenge. To circumvent excessive manual design and simple combination of different plasticity mechanisms, we introduce a more abstract level of plasticity: a parametric plasticity framework.

Adhering to the fundamental rule of local plasticity - that synaptic strength is influenced by pre- and post-synaptic neural activity - we design our framework based on a parametric expansion of the Spiking BCM rule [17]. The PDLF comprises two key components: Synaptic Cooperation Plasticity (SCP) and Presynaptic-Dependent Plasticity (PDP). SCP dynamically adjusts synaptic strength by considering the activity of both pre- and post-synaptic neurons. In contrast, PDP adjusts based on pre-synaptic activity alone and introduces a bias to synaptic changes for stability. The synaptic weight update in our framework is formulated as follows:

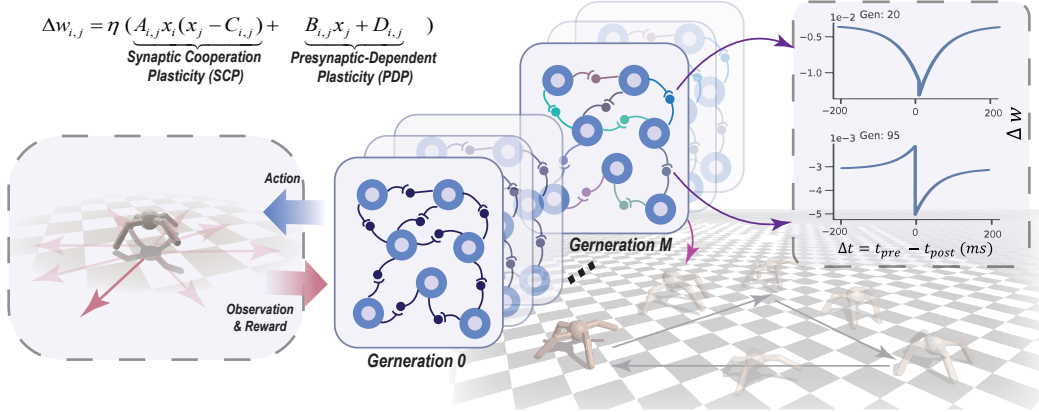


Figure 1: **Diagram of PDLF.** Top: By combining Synaptic Cooperation Plasticity (SCP) and Presynaptic-Dependent Plasticity (PDP), neurons can achieve diverse and heterogeneous plasticity. Bottom: Agents with PDLF learn plasticity rather than directly adjusting weights. Different forms of synaptic plasticity can be formed between neurons, enabling better multi-task learning. Plasticity helps the agents dynamically adjust weights and learn previously unseen scenarios during training, even without explicit reward signals.

$$\Delta w_{i,j} = \eta \left( \underbrace{A_{i,j}x_i(x_j - C_{i,j})}_{\text{Synaptic Cooperation Plasticity (SCP)}} + \underbrace{B_{i,j}x_j + D_{i,j}}_{\text{Presynaptic-Dependent Plasticity (PDP)}} \right) \quad (1)$$

In Eq. 1,  $\Delta w_{i,j}$  represents the change in synaptic weight between neurons  $i$  and  $j$ .  $x_i$  and  $x_j$  represent the spike traces [18] of pre- and post-synaptic neurons respectively. The parameters  $A_{i,j}$ ,  $B_{i,j}$ ,  $C_{i,j}$ , and  $D_{i,j}$  are learnable, enabling the network to form distinct and adaptable plasticity rules. SCP, represented by the term  $A_{i,j}x_i(x_j - C_{i,j})$ , adjusts synaptic strength based on the temporal correlation of neural activities, with  $C_{i,j}$  acting as a threshold for post-synaptic activity. PDP, denoted by  $B_{i,j}x_j + D_{i,j}$ , modifies synaptic weights based on pre-synaptic activity, with  $D_{i,j}$  providing a stable bias for each neuron. The learning rate  $\eta$  scales the overall synaptic weight change.

To optimize these parameters, we employ an Evolutionary Strategy (ES) [19], inspired by the natural selection processes shaping biological organisms. In this context, the parameters of the plasticity-centric learning rule can be viewed as intrinsic priors, optimized throughout the evolutionary process to ensure survival and adaptation. The ES involves a population of agents, each with a unique set of plasticity parameters, with their fitness evaluated based on adaptability and performance in various tasks. Through this process, the parameters are optimized, enabling agents to maintain flexible and dynamic adaptation throughout their lifespan.

## 2.2 PDLF Enhances Working Memory Capacity

In this section, we aim to demonstrate the effect of PDLF on Working Memory (WM). WM is the ability to maintain and process information temporarily and is the cornerstone of higher intelligence [20].

We explore the significant impact of PDLF on enhancing the WM capabilities of SNNs. We utilize a task known as the copying task [21], as illustrated in Fig. 2A. In this task, SNNs are initially presented with a sequence of stimuli, each lasting for 200 ms. This is then followed by a delay period of variable lengths, and finally, a test stimuli of equivalent duration to the sample stimuli is presented. The challenge for the SNNs lies in accurately reproducing the initial sequence of stimuli in the correct order upon receiving the test stimuli.

To thoroughly demonstrate the advantages of employing a PDLF-based approach in working memory tasks, we carry out a comparison with the strategy of directly optimizing weights utilizing the ES based on widely used three-layer SNNs. As shown in Fig. 2B, SNNs equipped with PDLF exhibit

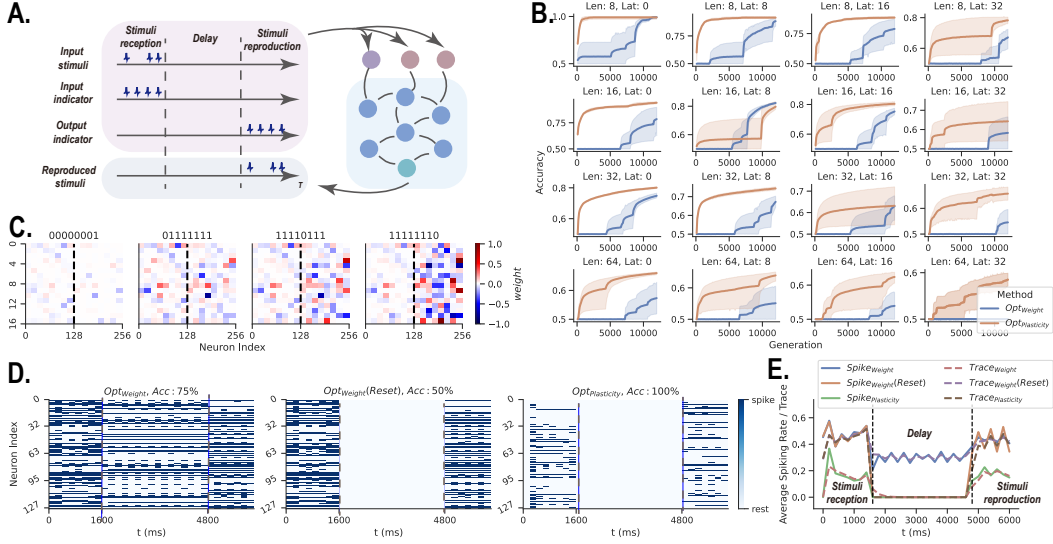


Figure 2: Design of the WM experiment and the impact of PDLF on WM. **A.** Schematic of the copying task. The SNNs first receive a sequence of motion stimuli, with each stimulus lasting 200 ms, followed by a delay period of varying lengths, and finally, a test stimulus of the same duration as the sample stimulus. The SNNs are required to reproduce the stimuli from the first phase to receive the test stimulus. **B.** Performance comparison between SNNs with plasticity and trained with direct weights. SNNs with plasticity show faster convergence, longer memory duration, and greater memory capacity. 'Len' refers to the length of stimulus samples, while 'Lat' refers to the number of steps in the delay period. **C.** Synaptic weights after different motion stimulus inputs when the number of motion samples is 8. SNNs with plasticity can form distinct connection weights for different stimuli. The left side of the dashed line shows the input weights associated with the stimulus, and the right side shows the output weights. **D.** Neuron states at different stages in SNNs trained directly with weights and those with PDLF. Directly trained SNNs require neural activity during the delay period to maintain memory. Resetting the membrane potential to 0 after the input stimulus leads to a chance-level memory accuracy, resulting in memory loss. In contrast, SNNs with plasticity can encode input stimuli into synaptic weights, demonstrating stronger memory functionality. **E.** Visualization of the firing rates at different stages and the average spike traces for SNNs using different strategies. SNNs with plasticity can maintain lower firing rates.

faster convergence rates, an ability to retain memory over longer durations, and an enhanced memory capacity.

To further investigate the influence of PDLF, we visualize synaptic weights following various stimuli inputs when the stimuli length is set to 8. As shown in Fig. 2C, SNNs endowed with PDLF can form distinct connection weights for different stimuli, demonstrating their superior adaptive capacity.

We compare the neuronal states at various stages between SNNs directly trained with weights and those incorporating PDLF, as illustrated in Fig. 2D. SNNs directly trained with weights rely on neuronal activity during the delay period to maintain memory. Resetting the membrane potential to 0 after the stimulus input leads to memory loss for input stimuli. This indicates that in SNNs directly optimized with weights, memory is primarily stored in neuronal activity. In contrast, SNNs incorporating PDLF encode the input stimulus into synaptic weights, demonstrating remarkable memory capabilities. Their ability to adjust synaptic weights facilitates the enhancement of working memory and allows neurons to remain in a resting state when not receiving task-related stimuli. This contributes to network efficiency and enhances network capacity, which has been validated in other biological and computational neuroscience studies [22; 23].

Finally, we visualize the average spike traces of SNNs under different training strategies, as shown in Fig. 2E. Notably, SNNs incorporating PDLF can sustain lower firing rates, thereby enhancing their efficiency in managing computational resources.

In summary, these results highlight the significant role of PDLF in bolstering the working memory capacity of SNNs, demonstrating its potential for facilitating complex cognitive tasks in artificial intelligence systems.

### 2.3 PDLF Enhances Multi-task Learning

Reinforcement Learning (RL) involves an agent learning to interact with its environment to achieve a specific goal, with the quality of its actions dictated by a reward signal. Conventional RL approaches often entail training the agent on a single task with a fixed reward function. However, in complex, real-world environments, agents need to handle multiple tasks and adjust to changing reward functions. This multi-task learning scenario presents significant challenges, mainly when the tasks involved are diverse and potentially conflicting.

In the field of RL, some of the most challenging problems lie within the domain of continuous control, usually modeled using sophisticated physics engines. These tasks require agents to manipulate simulated physical entities with high precision and coordination, similar to how humans control their limbs to carry out complex tasks. We use the Brax [24] simulator to design six continuous control environments. In these settings, agents need to navigate at various speeds, directions, and destination points. As shown in Fig. 3A, different task objectives are treated as observations to guide the agent in accomplishing different tasks. These challenging tasks serve as baselines in fields such as meta-learning [25; 26; 27]. During training, they are only exposed to a limited number of task instances, such as eight specific directions or eight fixed speeds. They use a single network to learn these unrelated or conflicting tasks.

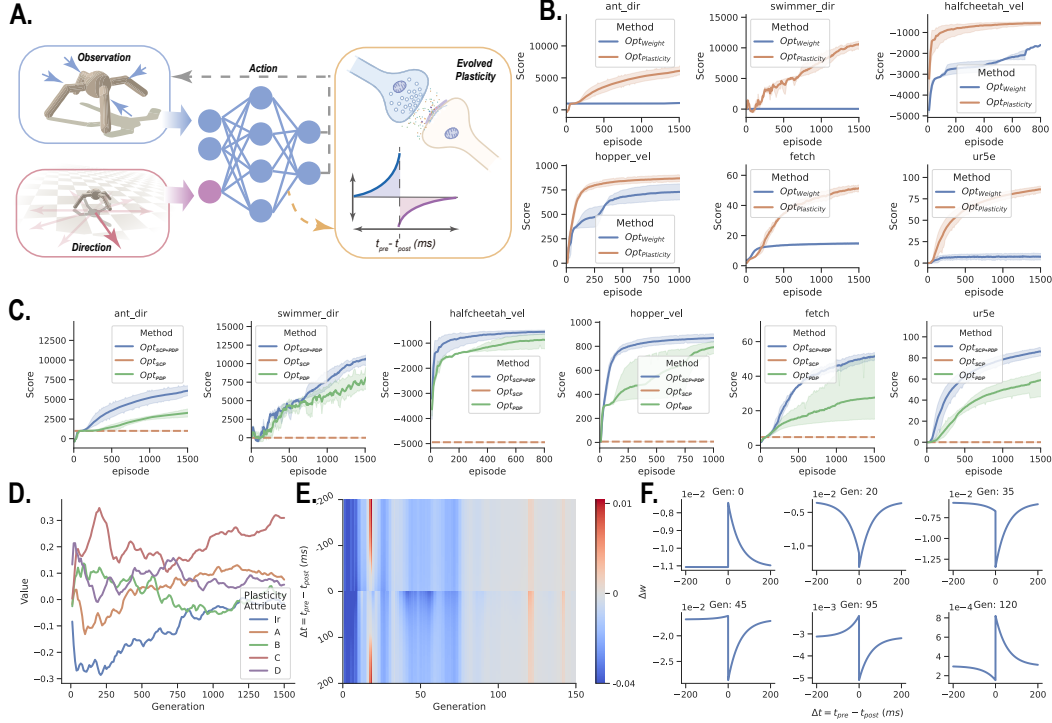
Our experiments compare two types of SNNs - one with synaptic weights that have been directly optimized and another with optimized PDLF. Both types of SNNs maintain the same scale and structure to ensure a fair comparison. Through this, we aim to highlight the advantages of optimizing PDLF over direct weight optimization in a multi-task environment. This comparison also evaluates the effectiveness and potential of our proposed model, especially in the face of the inherent challenges posed by complex continuous control tasks.

Table 1: Comparison of performance across various reinforcement learning tasks with different configurations of synaptic plasticity. Each task is evaluated using different training methods: Plasticity<sub>SCP+PDP</sub>, Plasticity<sub>SCP</sub>, Plasticity<sub>PDP</sub>, and direct weight training. The values presented are the mean and standard deviation over 5 trials. The row 'Chance Level' shows the performance metrics when randomly chooses actions. \* Upon the removal of Presynaptic-Dependent Plasticity (PDP), the SNNs become unstable, leading to divergence.

| Training               | ant_dir    | swimmer_dir | halfcheetah_vel | hopper_vel | fetch      | ur5e    |
|------------------------|------------|-------------|-----------------|------------|------------|---------|
| Opt <sub>SCP+PDP</sub> | 6904 ± 801 | 10531 ± 827 | -549 ± 95       | 869 ± 38   | 51 ± 3     | 86 ± 5  |
| Opt <sub>PDP</sub>     | 3284 ± 570 | 7831 ± 1479 | -870 ± 312      | 792 ± 50   | 26 ± 26    | 58 ± 13 |
| Opt <sub>SCP</sub> *   | -          | -           | -               | -          | -          | -       |
| Opt <sub>Weight</sub>  | 1069 ± 98  | 31 ± 8      | -1598 ± 324     | 729 ± 116  | 15 ± 0.6   | 7 ± 5   |
| Chance Level           | 995 ± 0.01 | 0.12 ± 0.02 | -4946 ± 1.3     | 6.51 ± 0.3 | 4.74 ± 0.0 | 0 ± 0.0 |

We explore the performance of PDLF in a three-layer, fully-connected SNN model with 128 hidden spiking neurons. Both the synaptic weights and the plasticity parameters are initialized to 0. During testing, their plasticity rules are fixed for agents with plasticity, and synaptic weights are reset to 0. The trained weights are applied during testing for agents trained directly on weights. We utilize reinforcement learning tasks to thoroughly test PDLF, requiring the agents to learn to cope with different tasks simultaneously and generalize the acquired knowledge to unseen, more complex tasks.

In our experiments, agents with PDLF show superior performance in multiple tasks compared to agents with directly optimized synaptic weights. As seen in Fig. 3B and Tab. 1, agents with PDLF exhibit more effective learning curves. The agents with PDLF quickly adapted to the changes in tasks, making them more capable of tackling the multi-task challenges inherent in the designed environments. In contrast, SNNs with directly trained weights fail to adapt to different tasks and can only acquire trivial solutions, such as maintaining approximate immobility in tasks involving multiple target directions.



**Figure 3: PDLF’s performance in multi-task reinforcement learning tasks and the influence of different plasticity attributes on performance.** **A.** Illustration of multi-task reinforcement learning. The agent is required to utilize a singular network to simultaneously learn multiple tasks with distinct objectives or even entirely opposing ones. The objectives of the tasks are treated as observations for the agent. They are inputted to the SNNs along with other observations such as joint positions, velocities, etc. **B.** Training curves of agents with PDLF versus those trained directly on weights. In these multi-task RL tasks, agents need to learn to move towards different directions (*ant\_dir*, *swimmer\_dir*), at varying speeds (*halfcheetah\_vel*, *hopper\_vel*), and to different locations (*fetch*, *ur5e*). Agents with PDLF maintain dynamic synaptic weights, learn characteristics of different tasks, and hence achieve superior performance in multi-task challenges. **C.** Ablation analysis of different plasticity mechanisms. Different colors represent training curves with some form of plasticity (SCP or PDP) removed. After removing PDP, SNNs diverge due to the loss of the equilibrium mechanism. Both SCP and PDP play significant roles in enhancing agent performance. **D.** The change curve of a synapse’s PDLF during the training process. Through evolutionary strategies, agents learn to adjust their plasticity. **E.** During the training process, at different inter-spike intervals of pre-synaptic and post-synaptic neurons, the impact of the plasticity of agents from different generations on weights. **F.** The specific functions of plasticity in agents from different generations as shown in **E**.

Ablation studies, depicted in Fig. 3C and Tab. 1, provide further insights into the contributions of different plasticity mechanisms. Removing any form of plasticity results in decreased agent performance, with the removal of PDP causing a divergence due to the loss of the equilibrium mechanism. This result highlights the importance of all plasticity mechanisms in maintaining the stability and adaptability of the agents.

The changing curve of a synapse’s PDLF during training (Fig. 3D), along with the impact of plasticity on weights for different generations of agents (Fig. 3E), demonstrate the effective learning of optimal parameters for the PDLF rule, facilitated by the evolutionary strategy. Interestingly, the specific functions of plasticity across different generations of agents differed (Fig. 3F), indicating the evolution and fine-tuning of plasticity mechanisms to improve agent performance across generations.

## 2.4 PDLF Enhances Generalization Ability

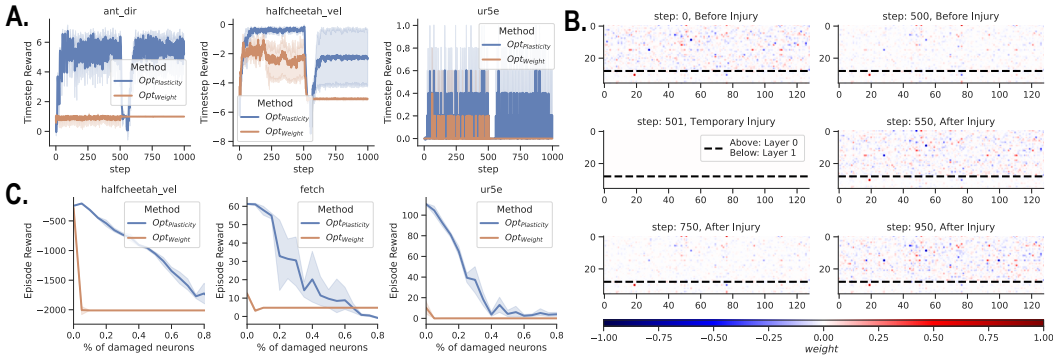


**Figure 4: Performance under temporary and permanent nerve injury.** **A.** The agent’s performance in the face of temporary neural damage. At the 500th step, all synaptic weights were reset to 0 to simulate a sudden neural system injury, and this condition lasted for 50 steps. Agents with plasticity were able to recover from this temporary loss, demonstrating better robustness. **B.** Network weights at different times before and after temporary damage. The synaptic weights of the input layer are shown above the dashed line, while the readout layer weights are below the dashed line. Even if the agent loses all synaptic weights due to temporary damage, it can still recover these weights based on its plasticity and input stimuli. **C.** The agent’s performance in the face of permanent neuronal damage of varying degrees. At the start of the test, neurons were blocked at different proportions, their synaptic weights set to 0, and could not be updated, simulating permanent neural network damage. Agents with plasticity performed better and exhibited stronger robustness when dealing with such permanent damage.

PDLF serves as an important mechanism for enhancing an agent’s generalization abilities, enabling the agent to exhibit stronger performance when dealing with unfamiliar tasks or when facing neuronal damage.

We further investigate the performance of PDLF when the agents faced injuries. We design two different types of injuries: temporary injuries and permanent injuries. Temporary injuries refer to a scenario where all synaptic weights of the agents are reset to 0 and kept for 50 steps. Permanent injuries refer to a situation where some synapses are set to 0 initially and do not update according to plasticity. In the tests for injuries, agents with plasticity display a remarkable ability to recover from temporary neuronal damage simulated by resetting all synaptic weights to 0 for 50 steps (Fig. 4A). Fig. 4B illustrates the changes in network weights at various stages before and after the temporary damage. Remarkably, despite losing all synaptic weights due to the inflicted temporary damage, agents manage to recover these weights using their inherent plasticity and incoming input stimuli. Moreover, even under permanent neuronal damage, with a proportion of neurons blocked and their weights unable to update, the plasticity-enabled agents continue to exhibit better performance and robustness (Fig. 4C). These results suggest that PDLF can contribute to the resilience of artificial agents, much as it does in biological systems.

More strikingly, agents with PDLF show a robust ability to generalize to tasks unseen during training, as demonstrated in Fig. 5A. For tasks with various movement directions and speeds, the agents only encounter a small subset of cases during training, represented by the red and orange points in Fig. 5A. Therefore, in this experiment, the agents are required to move in directions and at speeds unseen in training, emphasizing the agents’ more profound understanding and generalization capacity for the tasks. In contrast, agents trained directly on weights struggle with generalization due to their fixed weights during testing. This observation underscores the flexible adaptability offered by PDLF, enhancing the agent’s ability to navigate unseen scenarios.

During the training phase, the agents are instructed to move in straight lines in eight specific directions. However, as illustrated in Fig. 5A, agents with PDLF demonstrate a degree of generalization capability. They can learn to move in straight lines toward directions not encountered during training, while agents without PDLF struggle to generalize what they have learned.



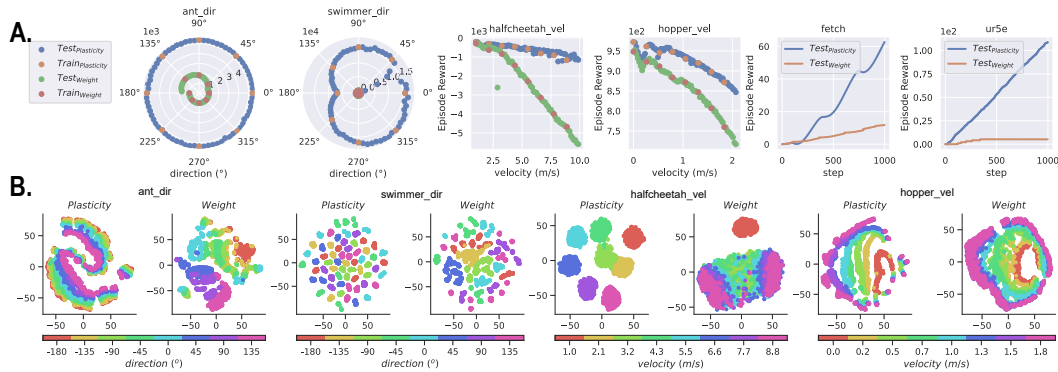


Figure 5: **A.** Performance of different agents in trained tasks and tasks not seen during training. Agents with plasticity can generalize well to unseen tasks, while agents trained directly on weights have difficulty generalizing to unseen test tasks due to their weights being fixed during testing. **B.** Low-dimensional embeddings of neuronal states during reinforcement learning tasks, differentiated by training strategy. Each point corresponds to the state of the hidden layer neurons at a specific time step. The color coding signifies distinct tasks. Agents that possess plasticity demonstrate an enhanced capability to distinguish between different tasks. Moreover, the neuronal states associated with identical tasks exhibit the intriguing property of forming a manifold within the high-dimensional space.

To further test the generalization capacity introduced by PDLF, we hope that agents could learn to turn or even form more complex paths simply by changing the target signal and without any additional feedback information related to posture. The results are shown in Fig. 6. Compared to agents that directly train their weights, those with PDLF demonstrate impressive generalization abilities toward this complex task. They can quickly adjust synaptic weights through PDLF and dynamically modify their state in previously unseen scenarios during different pieces of training. This allows them to progress toward varying target directions.

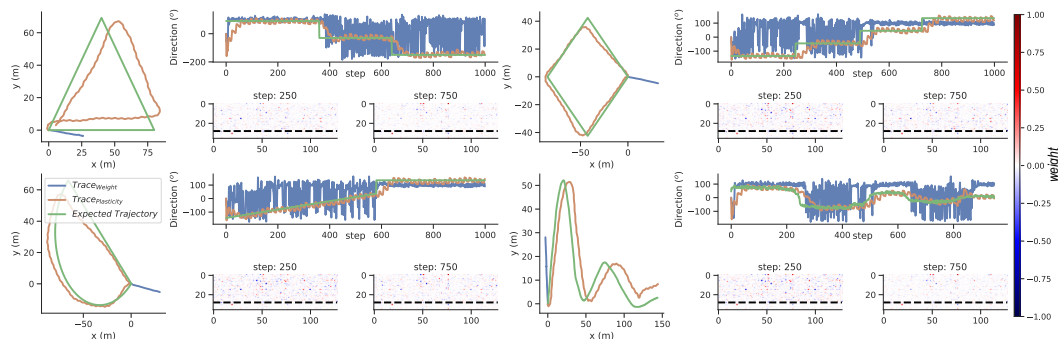


Figure 6: **Testing of the agent's generalization capabilities.** During training, the agent only learned to move in a straight line. The agent's movement trajectories are shown when the target direction is altered during the testing process. The green line represents the expected trajectory of the agent moving at a constant speed. The orange line is the actual movement trajectory of the agent with plasticity. Agents with plasticity can better understand different tasks, adjust synaptic weights according to different target directions, and thus show greater flexibility and superior generalization performance.

In Fig. 5B, we visualize the neuronal states of agents trained using different strategies during RL tasks in low-dimensional space. Each point in this representation corresponds to the state of the hidden layer neurons at a particular time step, with the varying colors indicating different tasks. The remarkable aspect of these visualizations is how agents with inherent plasticity demonstrate a



pronounced ability to discern between distinct tasks. Even more intriguing is the observation that the neuronal states corresponding to the same task tend to cluster together, forming a clear manifold in the high-dimensional space. This feature of PDLF contributes to the agent’s robust ability to generalize across various tasks while maintaining distinctive task-specific patterns in neuronal states. This further illustrates the powerful capabilities of agents with PDLF and the profound impact of such plasticity on the agent’s learning and adaptation abilities.

### 3 Discussion

Current artificial intelligence algorithms often focus on solving specific tasks, and their performance may fall short when faced with scenarios that deviate from their training conditions. These algorithms’ singular functionality, lack of robustness, and limited flexibility restrict their adaptability and application in complex and variable environments. In contrast, biological entities demonstrate exceptional adaptability in complex and changing environments, typically attributed to the plasticity of biological neural networks. Synaptic plasticity is the cornerstone and heart of exploring more generalized intelligence [28; 29].

SNNs with their brain-inspired operating mechanisms, lay the foundation for constructing flexible and robust intelligent systems, thereby attracting considerable attention in the field of artificial intelligence [30; 31; 32; 33]. However, current SNN training algorithms primarily rely on the backpropagation of external error signals and biologically-inspired plasticity rules, such as Spike-Timing-Dependent Plasticity. Although these methods demonstrate robust performance on individual tasks, the fixed learning paradigm still limits the generalization ability of SNNs and adaptability in multi-task environments. Contrary to the static nature of synaptic weight adjustments in traditional SNNs, we delve into PDLF, facilitated by the synergy between SCP and PDP. PDLF represents a higher-order learning process that dynamically adjusts plasticity rules. Through fostering adaptive synaptic modifications derived from the history of neuronal activity, PDLF promotes the emergence of a more dynamic and self-regulated learning system. Such a mechanism potentially narrows the gap between SNNs and their biological equivalents, thereby facilitating the progression towards continual learning and adaptation.

Our experimental results reveal that PDLF significantly enhances the memory capacity of SNNs by encoding memories directly into synaptic weights. Moreover, it does not rely on spike activity to sustain memory, allowing the network to remain in a resting state when not processing task-related stimuli, thus significantly improving the energy efficiency of SNNs. PDLF also dramatically amplifies the multi-task learning and generalization capabilities of SNNs, facilitating a swift transfer of knowledge learned from other tasks to more complex and unfamiliar tasks. Regarding adapting the paths and turning towards new directions, our PDLF models can maneuver in ways not encountered during training, a critical feature in complex, dynamic, and unpredictable real-world environments. Importantly, PDLF plays a pivotal role in bolstering the robustness of SNNs under simulated motor impairment scenarios. The exceptional resilience demonstrated in temporary damage scenarios validates the advantages of integrating PDLF into neural networks. Moreover, even in permanent damage, the exhibited resilience reinforces the case for PDLF as an inherent attribute of artificial systems. These characteristics reflect recovery mechanisms in biological systems where the brain mitigates damage through neural reorganization and the formation of new connections.

In conclusion, our study highlights PDLF as a critical feature that enhances the resilience and adaptability of artificial agents. These findings provide valuable insights for designing future artificial systems, opening up new possibilities for creating adaptive, robust, and intelligent agents capable of navigating complex and dynamic environments. Further work can explore more sophisticated forms of PDLF and study their impacts on various facets of artificial agent performance.

## 4 Method

### 4.1 Neuron and synaptic models

We employed leaky integrate-and-fire (LIF) neurons in our network models due to their biological plausibility and computational efficiency. The state of each LIF neuron was represented by its membrane potential, which integrated the incoming signals and generated a spike when the potential crossed a predefined threshold, as shown in Eq. 2.

$$\tau_m \frac{\partial v}{\partial t} = -(v - v_0) + I(t) \quad (2)$$

In Eq. 2,  $\tau_m$  is the membrane time constant,  $v$  is the membrane potential,  $v_0$  is the resting potential, and  $I(t)$  is the total synaptic current at time  $t$ . Once the membrane potential  $v$  exceeds a certain threshold  $v_{th}$ , the neuron generates a spike, and the potential is reset. A discrete form of the LIF neuron’s behavior can be described as:

$$\begin{aligned} u(t) &= v(t - \Delta t) + \frac{\Delta t}{\tau_m} \left( \sum_i w_i s_i(t) - v(t - \Delta t) + v_0 \right) \\ s(t) &= g(u(t) - v_{th}) \\ v(t) &= u(t)(1 - s(t)) + v_{reset}s(t) \end{aligned} \quad (3)$$

In Eq. 3,  $\Delta t$  is the time step,  $v_{reset}$  is the reset potential,  $u(t)$  and  $v(t)$  represent pre- and post-spike membrane potentials, and  $g(\cdot)$  is the Heaviside function modeling spiking behavior. After the loss of the reward signal, updating the network weights stops. This strategy of directly optimizing the weights is set as a control group in our experiments. Neuronal parameters are given in Tab. 2 unless otherwise specified.

*Traces* are the tracks produced at the pre- and post-synaptic sites by the spikes of pre- or post-synaptic neurons. Generally, these traces represent the recent activation level of pre- and post-synaptic neurons [18]. Traces can be computed by integrating spikes using a linear operator in the model and a low-pass filter in the circuit or by using non-linear operators/circuits. In the experiments, the synaptic traces were modeled as follows:

$$x(t) = \sum_{\tau=0}^t \lambda^{t-\tau} s(\tau) \quad (4)$$

In Eq. 4,  $x(t)$  is the synaptic trace at time  $t$ ,  $\lambda$  is the decay factor reflecting how quickly a spike’s influence fades with time, and  $s(\tau)$  represents the spike at time  $\tau$ . In the context of our experiment, these synaptic traces maintain a short-term history of neuron activation, thereby adding an element of temporal dynamics to our network model. As shown in Eq. 1, these synaptic traces are used to maintain a short-term history of neuronal activation and, in conjunction with PDLF, to modulate synaptic weights.

Table 2: Parameters of the spiking neurons.

| Parameter   | Value   |         | Description            |
|-------------|---------|---------|------------------------|
|             | WM task | RL task |                        |
| $\Delta t$  | 20 ms   | 200 ms  | Simulation time step   |
| $\tau_m$    | 40 ms   | 400 ms  | Membrane time constant |
| $\lambda$   | 54 ms   | 544 ms  | Decay factor           |
| $v_{th}$    | 0.1 V   | 0.1 V   | Membrane threshold     |
| $v_{reset}$ | 0 mV    | 0 mV    | Reset potential        |
| $v_0$       | 0 mV    | 0 mV    | Resting potential      |

## 4.2 Experimental Settings

### 4.2.1 Working Memory Task

To validate the impact of PDLF on working memory, we designed a working memory task. The agent would first receive a stimulus sequence, and after a delay of  $m$  steps, the agent is asked to reproduce the received stimulus. In each experiment, a random sequence of length  $n$  would be generated, where  $r_t \sim \mathcal{B}(1, \frac{1}{2})$ ,  $1 < t \leq n$ . At each time step, the input is a three-dimensional vector  $\vec{a}_t$ , which can be divided into three stages:

- **Stimulus reception:** If  $1 < t \leq n$ ,  $\vec{a}_t = (r_t, 1, 0)$ . The first element is the type of input stimulus, and the second element is the indicator for the input stimulus.
- **Delay:** If  $n + 1 < t \leq n + m$ ,  $\vec{a}_t = (0, 0, 0)$ . This phase represents a delay period where no new stimulus is presented.
- **Stimulus reproduction:** If  $n + m + 1 < t \leq 2n + m$ ,  $\vec{a}_t = (0, 0, 1)$ . The last element indicates whether a pulse needs to be reproduced.

At each step, the model has a scalar output  $s_t$ , which is a prediction for the stimulus. The Mean Square Error over the last  $m$  steps is taken as the reward of the model:

$$R = -\frac{1}{n} \sum_{\tau=1}^n (r_t - s_{m+n+\tau})^2 \quad (5)$$

Eq. 5 is used as a reward function in training. To intuitively compare agents with different strategies, as shown in Fig. 2B, we utilize the average accuracy per step as the performance measure during testing, as shown in Eq. 6.

$$\text{Acc} = \frac{1}{n} \sum_{\tau=1}^n (r_t == s_{m+n+\tau}) \quad (6)$$

During the stimulus reception stage, each stimulus follows the distribution  $\mathcal{B}(1, \frac{1}{2})$ , which means that the average accuracy at the chance level is 0.5.

#### 4.2.2 Multi-task Reinforcement Learning

We evaluated our method on five continuous control environments based on the Brax simulator (`ant_dir`, `swimmer_dir`, `halfcheetah_vel`, `hopper_vel`, `ur5e`, `fetch`).

- `ant_dir`: We train an ant agent to run in a target direction in this environment. The training task set includes 8 directions, uniformly sampled from  $[0, 360]$  degrees. As shown in Fig. 3D, the generalization test task set includes 72 directions, uniformly sampled from  $[0, 360]$  degrees. The agent’s reward comprises speed along the target direction and control cost.
- `swimmer_dir`: In this environment, we train a swimmer agent to move in a fixed direction. The settings for training and testing tasks are similar to `ant_dir`.
- `halfcheetah_vel`: In the `halfCheetah_vel` environment, we train a half-cheetah agent to move forward at a specific speed. The training tasks include 8 speeds, uniformly sampled from  $[1, 10]$  m/s. The generalization test tasks include 72 different speeds, uniformly sampled from the same range as the training tasks.
- `hopper_vel`: In the `hopper_vel` environment, we train a hopper agent to advance at a specific speed. The experimental setup is the same as `halfcheetah_vel`, but the sampling interval for the speed is  $[0, 2]$  m/s.
- `ur5e`: The UR5e is a common 6-DOF (degrees of freedom) robotic arm frequently used in industrial automation and robotics research. The agent receives a reward when the distance between the robotic arm’s end and the target position is less than 0.02 m. The target position is then randomly reset. The agent’s goal is to reach the target position as many times as possible within the stipulated time.
- `fetch`: We train a dog agent to run to a target location in this environment. The experimental setup is similar to `ur5e`.

The agent’s final reward is the average reward across all tasks, which encourages the agent to learn multiple tasks simultaneously.

---

**Algorithm 1** Parameter-Exploring Policy Gradients (PEPG)

---

- 1: Initialize the number of generations  $M$ , and the population size  $N$
  - 2: Initialize policy parameters  $\theta$
  - 3: Initialize adaptive noise scaling parameters  $\sigma$
  - 4: Initialize learning rates  $\alpha_\theta, \alpha_\sigma$
  - 5: Initialize Adam parameters  $m_\theta, v_\theta, m_\sigma, v_\sigma, \beta_1, \beta_2, \epsilon$
  - 6: Initialize noise standard deviation  $\sigma_0$
  - 7: **for**  $m = 1$  to  $M$  **do**
  - 8:     **for**  $n = 1$  to  $N$  **do**
  - 9:         Sample noise  $\epsilon \sim \mathcal{N}(0, \sigma_0)$
  - 10:         Compute offspring  $\theta' = \theta + \sigma \odot \epsilon$
  - 11:         Evaluate fitness  $f(\theta')$
  - 12:     **end for**
  - 13:     Compute fitness baseline  $b = \text{mean}(f(\theta'))$
  - 14:     Compute gradients  $\nabla_\theta = \frac{1}{N} \sum_{i=1}^N f_i \cdot \epsilon_i$
  - 15:     Compute adaptive noise scaling gradient  $\nabla_\sigma = \frac{1}{2N} \sum_{i=1}^N ((f_i - b)^2 - \sigma^2)$
  - 16:     Update Adam parameters for  $\theta$ :  $m_\theta = \beta_1 m_\theta + (1 - \beta_1) \nabla_\theta, v_\theta = \beta_2 v_\theta + (1 - \beta_2) \nabla_\theta^2$
  - 17:     Update policy parameters  $\theta = \theta + \alpha_\theta \cdot \frac{m_\theta}{\sqrt{v_\theta + \epsilon}}$
  - 18:     Update Adam parameters for  $\sigma$ :  $m_\sigma = \beta_1 m_\sigma + (1 - \beta_1) \nabla_\sigma, v_\sigma = \beta_2 v_\sigma + (1 - \beta_2) \nabla_\sigma^2$
  - 19:     Update adaptive noise scaling  $\sigma = \sigma \exp(\alpha_\sigma \cdot \frac{m_\sigma}{\sqrt{v_\sigma + \epsilon}})$
  - 20: **end for**
- 

Table 3: Parameters in PEPG.

| Parameter            | Value      | Description  |
|----------------------|------------|--|
| $\theta$             | 0          | Initial policy parameters                          |
| $\sigma$             | 0.1        | Initial adaptive noise scaling parameters          |
| $\alpha_\theta$      | 0.15       | Learning rate for policy parameters                |
| $\alpha_\sigma$      | 0.1        | Learning rate for adaptive noise scaling           |
| $m_\theta, v_\theta$ | 0, 0       | Initial Adam parameters for policy parameters      |
| $m_\sigma, v_\sigma$ | 0, 0       | Initial Adam parameters for adaptive noise scaling |
| $\beta_1, \beta_2$   | 0.9, 0.999 | Hyperparameters of Adam optimizer                  |
| $\epsilon$           | $10^{-8}$  | Adam parameters                                    |
| $M$                  | 1500       | Number of generations                              |
| $N$                  | 128        | Number of offspring per generation                 |

### 4.3 Training Strategies

We employ Parameter-Exploring Policy Gradients (PEPG) [19] to optimize SNNs. For SNNs with plasticity, the plasticity parameters in Eq. 1 are used for optimization. Evolution across generations is facilitated by modifying synaptic plasticity rules rather than directly adjusting the weights. SNNs with directly trained weights are considered a control group, where synaptic weights are the optimization parameters. The implementation of PEPG used in the experiments is provided by Algorithm 1. Unless expressly stated otherwise, the parameter settings and their explanations are shown in Table 3. The way to compute fitness  $f(\theta)$  varies depending on the task. For the working memory task, fitness is provided by Eq. 5, while for multi-task reinforcement learning, fitness is the average episodic reward across different subtasks.

### Data Availability

Codes and data have been deposited in GitHub <https://github.com/FloyedShen/PDLF> [34].

### References

- [1] Donald Olding Hebb. *The organization of behavior: A neuropsychological theory*. Psychology press, 2005.

- [2] Elie L Bienenstock, Leon N Cooper, and Paul W Munro. Theory for the development of neuron selectivity: orientation specificity and binocular interaction in visual cortex. *Journal of Neuroscience*, 2(1):32–48, 1982.
- [3] Guo-qiang Bi and Mu-ming Poo. Synaptic modifications in cultured hippocampal neurons: dependence on spike timing, synaptic strength, and postsynaptic cell type. *Journal of neuroscience*, 18(24):10464–10472, 1998.
- [4] Gina G Turrigiano. Homeostatic plasticity in neuronal networks: the more things change, the more they stay the same. *Trends in neurosciences*, 22(5):221–227, 1999.
- [5] Peter U Diehl and Matthew Cook. Unsupervised learning of digit recognition using spike-timing-dependent plasticity. *Frontiers in computational neuroscience*, 9:99, 2015.
- [6] Saeed Reza Kheradpisheh, Mohammad Ganjtabesh, and Timothée Masquelier. Bio-inspired unsupervised learning of visual features leads to robust invariant object recognition. *Neurocomputing*, 205:382–392, 2016.
- [7] Priyadarshini Panda and Kaushik Roy. Unsupervised regenerative learning of hierarchical features in spiking deep networks for object recognition. In *2016 international joint conference on neural networks (IJCNN)*, pages 299–306. IEEE, 2016.
- [8] Yu Duan, Zhongfan Jia, Qian Li, Yi Zhong, and Kaisheng Ma. Hebbian and gradient-based plasticity enables robust memory and rapid learning in rnns. *arXiv preprint arXiv:2302.03235*, 2023.
- [9] Wolfgang Maass. Networks of spiking neurons: the third generation of neural network models. *Neural networks*, 10(9):1659–1671, 1997.
- [10] David E. Rumelhart, Geoffrey E. Hinton, and Ronald J. Williams. Learning representations by back-propagating errors. 323(6088):533–536.
- [11] Yujie Wu, Lei Deng, Guoqi Li, Jun Zhu, and Luping Shi. Spatio-temporal backpropagation for training high-performance spiking neural networks. *Frontiers in neuroscience*, 12:331, 2018.
- [12] Timothy P Lillicrap, Adam Santoro, Luke Marris, Colin J Akerman, and Geoffrey Hinton. Backpropagation and the brain. *Nature Reviews Neuroscience*, 21(6):335–346, 2020.
- [13] Peter U Diehl and Matthew Cook. Unsupervised learning of digit recognition using spike-timing-dependent plasticity. *Frontiers in computational neuroscience*, 9:99, 2015.
- [14] Yiting Dong, Dongcheng Zhao, Yang Li, and Yi Zeng. An unsupervised stdp-based spiking neural network inspired by biologically plausible learning rules and connections. *Neural Networks*, 2023.
- [15] Dongcheng Zhao, Yi Zeng, Tielin Zhang, Mengting Shi, and Feifei Zhao. Glsnn: A multi-layer spiking neural network based on global feedback alignment and local stdp plasticity. *Frontiers in Computational Neuroscience*, 14:576841, 2020.
- [16] Julijana Gjorgjieva, Claudia Clopath, Juliette Audet, and Jean-Pascal Pfister. A triplet spike-timing-dependent plasticity model generalizes the bienenstock-cooper-munro rule to higher-order spatiotemporal correlations. *Proceedings of the National Academy of Sciences*, 108(48):19383–19388, 2011.
- [17] Trevor Bekolay, Carter Kolbeck, and Chris Eliasmith. Simultaneous unsupervised and supervised learning of cognitive functions in biologically plausible spiking neural networks. In *Proceedings of the annual meeting of the cognitive science society*, volume 35, 2013.
- [18] Jean-Pascal Pfister and Wulfram Gerstner. Triplets of spikes in a model of spike timing-dependent plasticity. *Journal of Neuroscience*, 26(38):9673–9682, 2006.
- [19] Frank Sehnke, Christian Osendorfer, Thomas Rückstieβ, Alex Graves, Jan Peters, and Jürgen Schmidhuber. Parameter-exploring policy gradients. *Neural Networks*, 23(4):551–559, 2010.

- [20] Alan D. Baddeley and Graham Hitch. Working memory. volume 8 of *Psychology of Learning and Motivation*, pages 47–89. Academic Press.
- [21] Sepp Hochreiter and Jürgen Schmidhuber. Long short-term memory. *Neural computation*, 9(8):1735–1780, 1997.
- [22] Gianluigi Mongillo, Omri Barak, and Misha Tsodyks. Synaptic theory of working memory. *Science*, 319(5869):1543–1546, 2008.
- [23] Nicolas Y Masse, Guangyu R Yang, H Francis Song, Xiao-Jing Wang, and David J Freedman. Circuit mechanisms for the maintenance and manipulation of information in working memory. *Nature neuroscience*, 22(7):1159–1167, 2019.
- [24] C. Daniel Freeman, Erik Frey, Anton Raichuk, Sertan Girgin, Igor Mordatch, and Olivier Bachem. Brax - a differentiable physics engine for large scale rigid body simulation, 2021.
- [25] Chelsea Finn, Pieter Abbeel, and Sergey Levine. Model-agnostic meta-learning for fast adaptation of deep networks, 2017.
- [26] Kaiyang Zhou, Ziwei Liu, Yu Qiao, Tao Xiang, and Chen Change Loy. Domain generalization: A survey. *IEEE Transactions on Pattern Analysis and Machine Intelligence*, 2022.
- [27] Julian Ibarz, Jie Tan, Chelsea Finn, Mrinal Kalakrishnan, Peter Pastor, and Sergey Levine. How to train your robot with deep reinforcement learning: lessons we have learned. *The International Journal of Robotics Research*, 40(4-5):698–721, 2021.
- [28] Xu Liu, Steve Ramirez, Petti T Pang, Corey B Puryear, Arvind Govindarajan, Karl Deisseroth, and Susumu Tonegawa. Optogenetic stimulation of a hippocampal engram activates fear memory recall. *Nature*, 484(7394):381–385, 2012.
- [29] Stephen J Martin, Paul D Grimwood, and Richard GM Morris. Synaptic plasticity and memory: an evaluation of the hypothesis. *Annual review of neuroscience*, 23(1):649–711, 2000.
- [30] Paul A Merolla, John V Arthur, Rodrigo Alvarez-Icaza, Andrew S Cassidy, Jun Sawada, Filipp Akopyan, Bryan L Jackson, Nabil Imam, Chen Guo, Yutaka Nakamura, et al. A million spiking-neuron integrated circuit with a scalable communication network and interface. *Science*, 345(6197):668–673, 2014.
- [31] Mike Davies, Narayan Srinivasa, Tsung-Han Lin, Gautham Chinya, Yongqiang Cao, Sri Harsha Choday, Georgios Dimou, Prasad Joshi, Nabil Imam, Shweta Jain, et al. Loihi: A neuromorphic manycore processor with on-chip learning. *Ieee Micro*, 38(1):82–99, 2018.
- [32] Jing Pei, Lei Deng, Sen Song, Mingguo Zhao, Youhui Zhang, Shuang Wu, Guanrui Wang, Zhe Zou, Zhenzhi Wu, Wei He, et al. Towards artificial general intelligence with hybrid tianjic chip architecture. *Nature*, 572(7767):106–111, 2019.
- [33] Maxence Bouvier, Alexandre Valentian, Thomas Mesquida, Francois Rummens, Marina Reyboz, Elisa Vianello, and Edith Beigne. Spiking neural networks hardware implementations and challenges: A survey. *ACM Journal on Emerging Technologies in Computing Systems (JETC)*, 15(2):1–35, 2019.
- [34] Shen Guobin, Zhao Dongcheng, and Zeng Yi. Metaplasticity: Unifying learning and homeostatic plasticity in spiking neural networks, 2023.